THE JOURNAL OF PHYSICAL CHEMISTRY LETTERS
A JOURNAL OF THE AMERICAN CHEMICAL SOCIETY

pubs.acs.org/JPCL

Letter

Cation-Driven Lipopolysaccharide Morphological Changes Impact Heterogeneous Reactions of Nitric Acid with Sea Spray Aerosol Particles

Christopher Lee,[§] Abigail C. Dommer,[§] Jamie M. Schiffer, Rommie E. Amaro, Vicki H. Grassian, and Kimberly A. Prather*

Cite This: *J. Phys. Chem. Lett.* 2021, 12, 5023−5029

Read Online

ACCESS | Metrics & More | Article Recommendations | Supporting Information

ABSTRACT: Lipopolysaccharides (LPS) in sea spray aerosol (SSA) particles have recently been shown to undergo heterogeneous reactions with HNO_3 in the atmosphere. Here, we integrate theory and experiment to further investigate how the most abundant sea salt cations, Na^+, Mg^{2+}, and Ca^{2+}, impact HNO_3 reactions with LPS-containing SSA particles. Aerosol reaction flow tube studies show that heterogeneous reactions of SSA particles with divalent cation (Mg^{2+} and Ca^{2+}) and LPS signatures were less reactive with HNO_3 than those dominated by monovalent cations (Na^+). All-atom molecular dynamics simulations of model LPS aggregates suggest that divalent cations cross-link the oligosaccharide chains to increase molecular aggregation and rigidity, which changes the particle phase and morphology, decreases water diffusion, and consequently decreases the reactive uptake of HNO_3. This study provides new insight into how complex chemical interactions between ocean-derived salts and biogenic organic species can impact the heterogeneous reactivity of SSA particles.

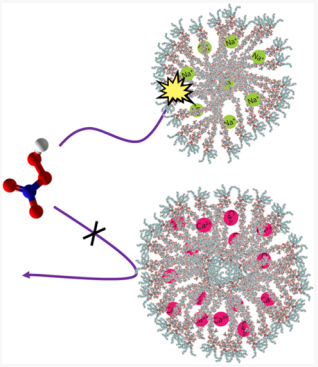

Sea spray aerosol (SSA) particles are one of the most abundant naturally produced aerosols in our atmosphere. Yet, their heterogeneous reactivity in the atmosphere is not well-understood as chemically simple systems have only been investigated.[1−4] Understanding the heterogeneous reactivity of SSA particles is important for water uptake and cloud formation which is key to controlling our climate and reducing one of the greatest uncertainties in current climate models.[5] SSA particles are composed of a wide array of inorganic and organic components, ranging from simple mixtures of sea salt to entire microbial cells.[6−8] The composition of each SSA particle impacts its climate-relevant properties, including the interaction with gas phase species like HNO_3 that are important for regulating nitrogen levels in the global nitrogen cycle.[9] Up to 63.9% of SSA particles with aerodynamic sizes greater than 1 μm (supermicron SSA) contain polysaccharide signatures, including lipopolysaccharides (LPS), as determined from Raman microspectroscopy.[8] Recently, LPS species have been shown to undergo acid−base reactions with HNO_3 in SSA particles, changing the paradigm of heterogeneous reaction between SSA and HNO_3 involving only inorganic species.[3,10]

LPS is a major component of outer-cell membranes of Gram-negative bacteria, known constituents of microbial life within the sea surface microlayer, and a source of SSA components. The chemical structure of LPS, which primarily protects microbial cells, is expected to also impact SSA reaction pathways. Each LPS molecule is composed of three parts, i.e., (1) Lipid A, (2) inner and outer core oligosaccharides, and (3) repeating O-antigens, a repetitive glycan polymer (Scheme 1).[11,12] Upon reaction with HNO_3, LPS can undergo acid−base chemistry by becoming protonated at the carboxylate and phosphate groups located within the inner and outer core oligosaccharides. This reaction process displaces coordinating cations (i.e., sodium, calcium, magnesium). The significance of this heterogeneous reaction pathway in nascent SSA particles was recently established through single-particle studies by Raman microspectroscopy and aerosol time-of-flight mass spectrometry (ATOFMS).[10]

Different cations are known to elicit unique morphological properties in LPS monolayers and bilayers.[13−16] Coughlin et al. reported that purified sodium LPS salt forms tube-like aggregates, while the presence of divalent cations calcium or magnesium induces the formation of LPS bilayer aggregates.[14,15] Many studies have also noted that the high activity of divalent cations leads to the displacement of monovalent cations weakly bound to the saccharide headgroups, with calcium binding more tightly relative to magnesium.[13,15−18] The striking sensitivity of LPS aggregate morphology to cation type, and the high preference for calcium binding, has also

Received: March 12, 2021
Accepted: May 6, 2021
Published: May 22, 2021

https://doi.org/10.1021/acs.jpclett.1c00810
J. Phys. Chem. Lett. 2021, 12, 5023−5029

Scheme 1. (A) Glycan Symbol Representation of Model LPS Used in This Study. (B) Hard-sphere Atomic Model of LPS Corresponding to the Diagram in (A).[a]

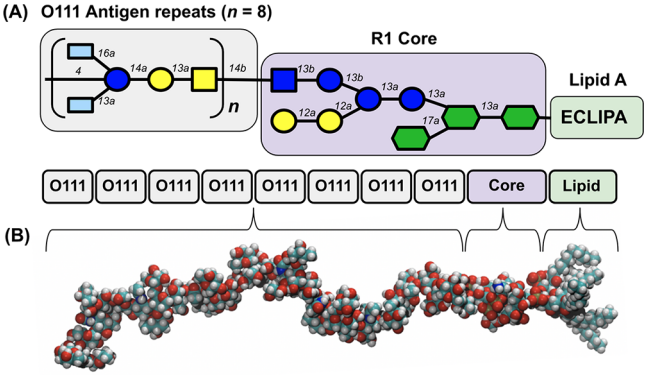

[a]Colorcode: white, hydrogen; teal, carbon; red, oxygen; blue, nitrogen; tan, phosphorous. Detailed chemical structure can be found in Trueblood et al.[6]

been associated with the resistance of bacteria to commercial sanitizers; calcium is suggested to cross-link the saccharide chains together, preventing membrane penetration by the weaker cationic surfactants used in sanitizers.[13] A similar mechanism may play a role in the reactive uptake of trace atmospheric gases by marine aerosols, but the specific impacts of cation type on LPS-transformed SSA particle morphology and reactivity remain unclear.

Here, we sought to understand the specific impact of monovalent and divalent cations on heterogeneous reactions between LPS-transformed SSA particles and HNO_3. Both simplified salt-LPS model aerosols as well as nascent aerosols generated from a laboratory-induced phytoplankton bloom were investigated. ATOFMS was used to reveal how cation valency drives LPS physicochemical changes in the aerosol phase, which in turn impacts the aerosol heterogeneous reactivity toward HNO_3.[19] Furthermore, explicit solvent all-atom molecular dynamics simulations of LPS bilayers under different cation conditions were performed to provide a molecular-level explanation of the reactivity behavior.[4] Taken together, these findings can provide substantial insight into the molecular mechanisms behind cation-driven LPS morphology, phase, and correlated reactivity.[20,21]

Chemical changes in LPS-containing SSA particles were investigated during the Investigation into Marine Particle Chemistry and Transfer Science (IMPACTS) campaign, where a phytoplankton bloom was induced using natural Pacific

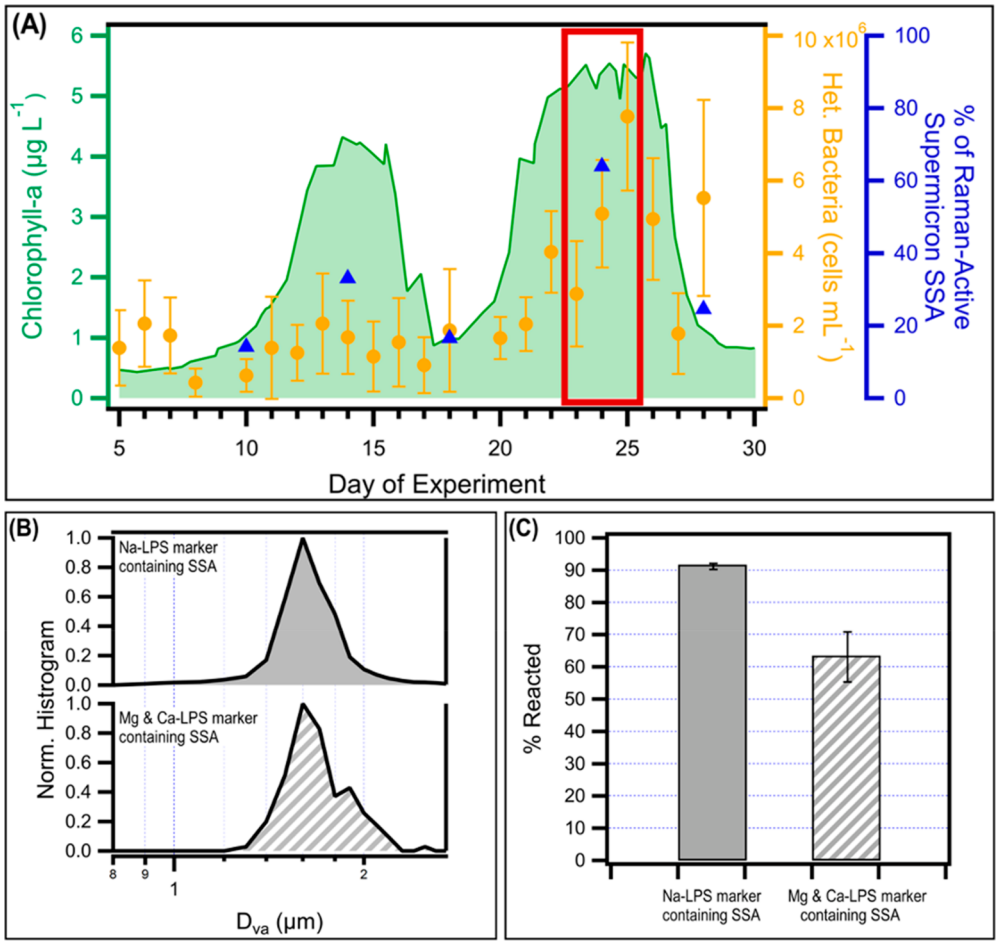

Figure 1. (A) Seawater chlorophyll-a (green) and heterotrophic bacteria concentrations (orange) with the percentage of SSA-containing polysaccharides, including LPS[6] (blue), over the course of the phytoplankton blooms from the IMPACTS campaign. Period of supermicron SSA polysaccharide-enrichment for further ATOFMS data analysis is noted by the red box. (B) ATOFMS size histogram of Na-LPS (solid fill) and Mg/Ca-LPS SSA (dashed fill) from the IMPACTS campaign. (C) Percentage of reacted Na-LPS (solid fill) and Mg/Ca-LPS SSA (dashed fill) detected by ATOFMS with HNO_3 reaction flow tube from the IMPACTS 2014 campaign. Error bars in (C) represent 2σ for the 95% confidence limit.

https://doi.org/10.1021/acs.jpclett.1c00810
J. Phys. Chem. Lett. 2021, 12, 5023−5029

Ocean seawater.[7,8] The induced bloom in the ocean-atmosphere interaction facility (OAIF) produced SSA particles that are representative of those produced over the ocean at varying biological activities.[7,22] While two phytoplankton blooms were induced from the same seawater during the IMPACTS campaign (Figure 1A, green trace),[7] we focus on the second phytoplankton bloom in the study due to the concurrent bloom of heterotrophic bacteria (Figure 1A, orange marker) in the seawater as well as high enrichment of polysaccharides in the supermicron SSA population (Figure 1A, blue marker) as identified using Raman spectroscopic analysis by Cochran et al.[8] As each day contains data from tens to hundreds of thousands of particles, we further zoom into a single day during the second bloom (Figure 1A, red box) where 63.9% of the Raman-active supermicron SSA particles contain polysaccharides.

Using known LPS ion markers from reference ATOFMS mass spectra of LPS (Figure S1), we isolated 5011 LPS-containing SSA particles out of a total of 52918 particles (10.6 ± 0.3%) for 1 day of the study. Two types of particles were observed, i.e., (1) LPS-containing SSA with a dominant sodium signal (herein referred as Na-LPS SSA) and (2) LPS-containing SSA with dominant Mg and Ca signals (>10% rel. area intensity of $^{24}Mg^+$ or $^{40}Ca^+$, herein referred as Mg/Ca-LPS SSA), where these particles made up 98.0 ± 0.4% and 42.0 ± 2.2% of the total LPS-containing SSA particles, respectively. In these SSA particles, Mg/Ca-LPS SSA particles exhibited a more pronounced second peak in the larger aerodynamic sizes at 1.9 μm D_{va} (vacuum aerodynamic diameter, herein referred to as aerodynamic diameter) compared to Na-LPS SSA particles (Figure 1B). This can be attributed to either an increase in particle size or change in shape as ATOFMS measures the particles' aerodynamic diameter and a change in shape leads to an apparent change in aerodynamic diameter.[23] Ultimately, when these particles were reacted with 350 ppb HNO_3 at 60 ± 2% relative humidity (RH), a lower percentage of Mg/Ca-LPS SSA particles reacted (63.6 ± 8.1%) than Na-LPS SSA particles (91.7 ± 0.8%) (Figure 1C). Given the level of chemical complexity of nascent SSA particles, we hypothesize that this shift in size and the associated differences in heterogeneous reactivity are due to aggregation of the LPS molecules with divalent cations that are enriched at the air–water interface of SSML and ejected as SSA particles.[24−27] We sought to investigate the role of cation valency using a more controlled model system consisting of specific salts and LPS using a synergistic experimental and computational approach.

Model systems of salt-LPS particles were produced by atomizing LPS solutions containing different countercations, namely, Na^+, Mg^{2+}, and Ca^{2+}. The ATOFMS, which provides size-resolved, dual-polarity mass spectra of single particles,[19] can detect single soluble and insoluble particles, as well as agglomerates of different particles across a wide size range (Figure S2).[28] As done in the analysis of the IMPACTS campaign, select ion markers of LPS, obtained from a reference mass spectrum (Figure S1), were used to isolate particles containing LPS from the total population of atomized LPS particles. In the model systems, the generated aerosols are called LPS particles to easily distinguish this system with the complex system of the IMPACTS campaign.

In this study, we determined that morphology and particle size of LPS particles depends upon the countercation present. Results from ATOFMS on these model LPS particles revealed a more pronounced shift from predominantly submicrometer (submicron) to supermicrometer (supermicron) sizes depending upon the countercation present (Figure 2). This is

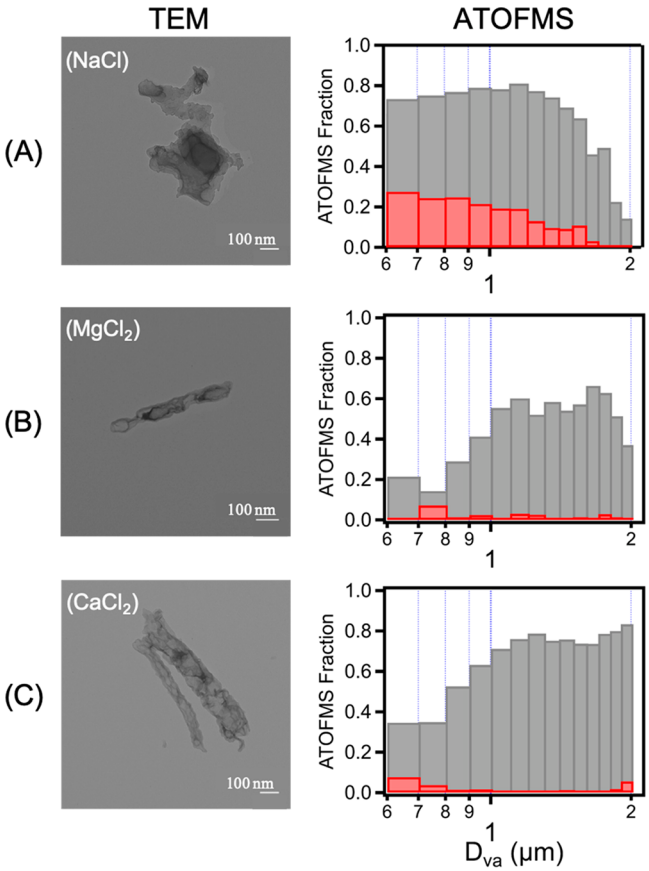

Figure 2. (Left) Transmission electron microscope images of negative-stained atomized particles, and (right) normalized size distribution of LPS particles detected by ATOFMS for (A) LPS spiked with 0.010 M NaCl, (B) LPS spiked with 0.010 M $MgCl_2$, and (C) LPS spiked with 0.010 M $CaCl_2$. Scale bar on the image denotes 100 nm; the ATOFMS total LPS particles are shown in gray, whereas the reacted LPS particles are overlaid in red.

consistent with observations made during IMPACTS. Na-LPS particles were predominantly in the submicron size range, whereas Mg- and Ca-LPS particles were in the supermicron range. In order the visualize the physical changes, we took transmission electron microscopy (TEM, FEI Tecnai Spirit) images of the negative-stained[29,30] atomized LPS particles and revealed that Na-LPS particles exhibited long tubular structures of a single-layered structure, whereas Mg- and Ca-LPS particles exhibited bilayer sheets as previously observed in a study that characterized the LPS salts in bulk solution using TEM.[14]

It is unclear how this change in the morphology impacts the heterogeneous reactivity of SSA particles in the atmosphere. To investigate this, we reacted these model LPS particles in an aerosol flow tube using 10 ppb HNO_3 at 50 ± 2% RH, a lower and more atmospherically relevant condition.[31] These simple model LPS particles showed very similar behavior to the complex SSA in Figure 1C. Na-LPS particles were more ∼8 times more reactive with HNO_3 (24.1 ± 1.3%) compared to Mg- (2.5 ± 0.8%) or Ca-LPS (3.7 ± 1.2%) particles. These results all converge to support our original hypothesis that changes in LPS-cation structures formed with different

https://doi.org/10.1021/acs.jpclett.1c00810
J. Phys. Chem. Lett. 2021, 12, 5023−5029

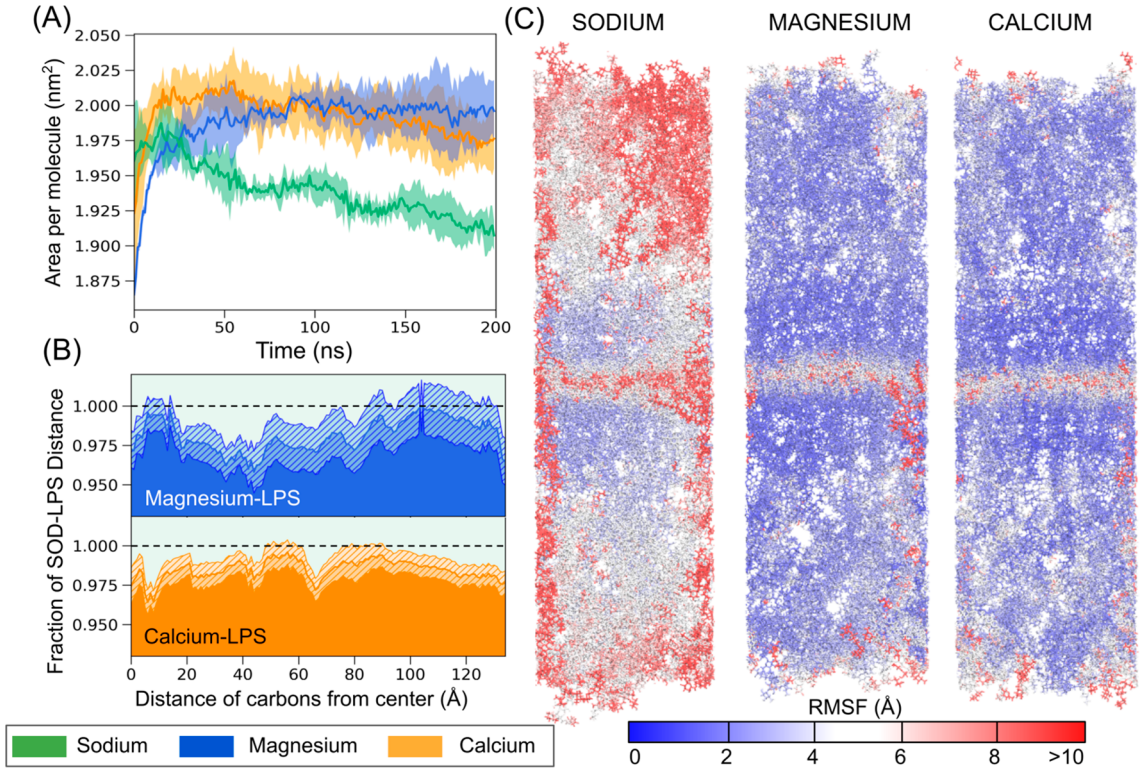

Figure 3. (A) Area per molecule (APM) measurements in nm^2 LPS-$molecule^{-1}$ over each 200 ns trajectory. Replicates are indicated by average area per molecule over time with the standard deviation shaded above and below, with Ca-LPS in orange, Na-LPS in green, and Mg-LPS in blue. (B) LPS chain length fractions of Mg-LPS (top) and Ca-LPS (bottom) as fractions of Na-LPS chain length. Error propagation bars are given by hatches. Dotted lines indicate unity. (C) Atomic-level root-mean-square fluctuations (RMSF) were calculated over the final 50 ns of simulation for replicates of Na-LPS (left), Mg-LPS (center), and Ca-LPS (right) bilayers. Atoms are colored by RMSF value, with red indicating more fluctuations and blue indicating less fluctuations. Note that red atoms located at the edges of the simulation box may be due to artifacts of molecules moving across periodic boundaries and not corrected by the gmx rmsf module.

countercations present can change the atmospheric reactivity of SSA particles.

LPS molecules tend to form bilayer aggregates in the presence of different divalent countercations as observed here and in previous studies (Figure 2).[14,32] To understand how these higher order LPS structures could alter heterogeneous pathways at the atomic level, we performed three all-atom explicit solvent molecular dynamics simulations of an *E. coli* O111 LPS bilayer, the same LPS structure used in these model experiments. CHARMM-GUI was used to construct the model systems with coordinating cations.[33−35] Each LPS molecule contained eight O-antigen repeating units, an R1 core, and Lipid A, and each was conjugated to Mg^{2+}, Ca^{2+}, or Na^+ countercations to balance the charges.

To elucidate the impact of the countercation on LPS bilayer structure, we compared the equilibrium area per molecule and LPS chain length and orientations. The simulations show that, under constant pressure, the LPS bilayer in Ca^{2+} and Mg^{2+} matrices expanded laterally in area from their initial postequilibration structures, while LPS in Na^+ matrix contracted laterally. Figure 3A shows how this expansion is reflected in the area per molecule of the LPS bilayers over the duration of each molecular dynamics trajectory. On average, the final area per molecule of Na-LPS molecules (1.91 ± 0.01 nm^2) was markedly lower than that of both Ca- and Mg-LPS (1.98 ± 0.02 and 2.01 ± 0.02 nm^2, respectively). Additionally, in both divalent cation matrices, the LPS chains underwent vertical compression compared to their Na-complexed LPS counterparts. In direct comparisons between monosaccharide units in Ca- or Mg-LPS chains with Na-LPS chains, both calcium and magnesium cations induced crunching in the oligosaccharides, resulting in chain lengths consistently shorter than those of Na-LPS (Figure 3B). This observation is in line with previous work, which has documented the calcium-induced collapse of monolayers containing LPS isolated from *Pseudomona aeruginosa*.[36]

To understand the impacts of cation valency on the LPS aggregate dynamics, we compared the atomic-level root-mean-square fluctuations (RMSF). RMSF calculations indicate that the O-antigen chains on Na-LPS exhibited a much higher degree of flexibility than those complexed with magnesium or calcium, which adopted a more rigid structure (Figure 3C). These calculations are in line with experimentally measured compressibilities for salt-LPS monolayers, where Na-LPS monolayers demonstrate high compressibility compared to Ca-LPS.[37] However, the impacts of cation type on the core region flexibility of the LPS molecules is much less pronounced, indicating that specific cation interactions within the saccharide chains are more impactful to the overall dynamics of LPS bilayers than interactions with the R1 core or Lipid A.

To understand how the morphological changes in the LPS bilayer impact the reactivity of the LPS aggregate, we calculated the water diffusion coefficients and water density for each system. The diffusivity of water throughout the LPS when complexed to sodium was significantly higher than when complexed to magnesium or calcium (Figure 4A). Additionally, measurements of water density throughout the bilayers

https://doi.org/10.1021/acs.jpclett.1c00810
J. Phys. Chem. Lett. 2021, 12, 5023−5029

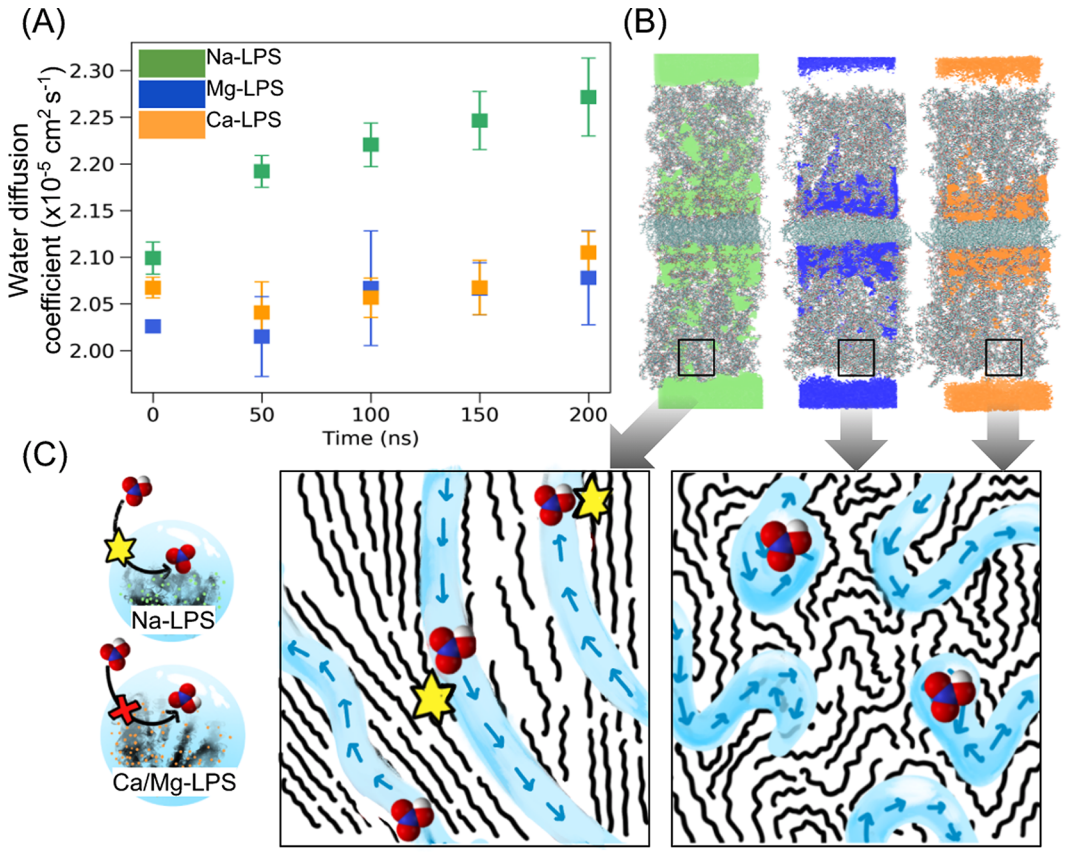

Figure 4. (A) Water diffusion coefficients of LPS bilayers complexed to either sodium (green), magnesium (blue), or calcium (orange). (B) Water density measurements for replicate 1 of each countercation averaged over the entire 200 ns trajectory. Water is visualized by color, where Na-LPS is given by green, Mg-LPS is given by blue, and Ca-LPS is given by orange volume maps, overlaid by corresponding LPS molecules. (C) Schematic representing how water diffusion impacts HNO_3 reactivity based on structural changes in the LPS molecules.

indicate that water molecules in the Na LPS bilayers were able to occupy space between the O-antigen regions of the LPS molecules. Conversely, the water in Ca/Mg LPS bilayers is mainly concentrated in the core region of the LPS (Figure 4B). The dehydration of the saccharide regions as indicated by low water occupation and diffusion constants in Ca/Mg LPS bilayers likely accounts for the reduced HNO_3 reactivity of these LPS particle types, as the morphology of these Ca/Mg LPS particles prevents diffusion of dissolved HNO_3 into the LPS core where it can undergo protonation reactions at the phosphate and carboxylate sites.

One possible explanation for the cation-dependent differences in morphology and reactivity of LPS bilayers is that divalent cations, by chelating two singly charged reactive sites each, deform the structures of the oligosaccharides while positioning them into ideal cross-linking conformations, which simultaneously dehydrates the O-antigen regions and blocks the movement of water.[13,15,16,36,37] Monovalent sodium cations do not appear to significantly disrupt the alignment of the LPS molecules; however, divalent cations induce structural deformation away from the bilayer normal in the oligosaccharide chains, which increases the molecular footprint of each LPS molecule and causes the bilayer to expand. Notably, the increase in area per molecule does not correspond to an increase in water diffusion throughout aggregate; rather, the LPS conformations hinder water diffusion by forming a relatively dehydrated and intertwined network of saccharide chains, also known as microgels, which have been observed in marine environments.[38] Although the Na-LPS bilayer adopts a lower area per molecule, the lower specificity of the saccharide chains to sodium and the alignment of the molecules allows for greater molecular flexibility. This more flexible structure promotes the diffusion of water and small molecules such as nitric acid, which increases the overall heterogeneous reactivity of Na-LPS aggregates compared to the divalent analogs.

SSA particles have been shown to exhibit a wide range of heterogeneous reactivities at the single-particle level.[1,39] Results from this study provide a detailed atomic-level examination of the factors that helps explain the observed variation in reactivity in LPS-containing SSA particles. Specifically, cation type elicits differences in physicochemical properties of LPS-containing marine aerosols, highlighting the role that countercations play on aerosol structure and atmospheric reactivity. This discovery has important implications not only for other atmospheric heterogeneous reactions including oxidation reactions but also in key surface processes such as water uptake, cloud droplets, and ice nucleation.[40−44] This study demonstrates how the addition of biogenically derived LPS molecules can impact SSA physicochemical properties and reactivity, warranting further investigations into how these morphological changes impact relevant properties including cloud and ice forming abilities.

https://doi.org/10.1021/acs.jpclett.1c00810
J. Phys. Chem. Lett. 2021, 12, 5023−5029

■ ASSOCIATED CONTENT

Supporting Information

are given in the Supporting Information. . The Supporting Information is available free of charge at https://pubs.acs.org/doi/10.1021/acs.jpclett.1c00810.

Further information on the experiment methods and setup, size distribution of atomized LPS particles, and ATOFMS data showing the averaged mass spectra of LPS particles and molecular dynamics simulations (PDF)

■ AUTHOR INFORMATION

Corresponding Author

Kimberly A. Prather − *Scripps Institution of Oceanography, University of California San Diego, La Jolla, California 92037, United States; Department of Chemistry and Biochemistry, University of California San Diego, La Jolla, California 92093, United States*; Email: kprather@ucsd.edu

Authors

Christopher Lee − *Scripps Institution of Oceanography, University of California San Diego, La Jolla, California 92037, United States;* orcid.org/0000-0002-5329-9750

Abigail C. Dommer − *Department of Chemistry and Biochemistry, University of California San Diego, La Jolla, California 92093, United States;* orcid.org/0000-0003-4847-4136

Jamie M. Schiffer − *Department of Chemistry and Biochemistry, University of California San Diego, La Jolla, California 92093, United States;* Present Address: Takeda Pharmaceuticals, San Diego, California 92121, United States of America (J.M.S.); orcid.org/0000-0002-0208-6958

Rommie E. Amaro − *Department of Chemistry and Biochemistry, University of California San Diego, La Jolla, California 92093, United States;* orcid.org/0000-0002-9275-9553

Vicki H. Grassian − *Department of Chemistry and Biochemistry, University of California San Diego, La Jolla, California 92093, United States;* orcid.org/0000-0001-5052-0045

Complete contact information is available at: https://pubs.acs.org/10.1021/acs.jpclett.1c00810

Author Contributions

§C.L. and A.C.D. contributed equally.

Notes

Data Availability: All data and IPython notebooks for this work are available as part of the UCSD Library Digital Collections (10.6075/J0862F04 and https://library.ucsd.edu/dc/collection/bb96275693).

The authors declare no competing financial interest.

■ ACKNOWLEDGMENTS

This work is funded by NSF Center for Aerosol Impacts on Chemistry of the Environment (CAICE), National Science Foundation Center for Chemical Innovation (NSF CHE-1801971). Computing support through XSEDE was provided by NSF CHE-060073N to R.E.A. The authors would like to thank all collaborators involved with the NSF CAICE IMPACTS intensive campaign and the Scripps Institution of Oceanography Hydraulic Laboratory staff. The authors thank O. Ryder, M. Santander, and J. Dowling for their valuable contributions and G. Castillon, M. Ellisman, and the National Center of Microscopy and Imaging Research for the TEM component of this study.

■ REFERENCES

(1) Abbatt, J. P. D.; Lee, A. K. Y.; Thornton, J. A. Quantifying Trace Gas Uptake to Tropospheric Aerosol: Recent Advances and Remaining Challenges. *Chem. Soc. Rev.* **2012**, *41* (19), 6555.

(2) Bertram, T. H.; Cochran, R. E.; Grassian, V. H.; Stone, E. A. Sea Spray Aerosol Chemical Composition: Elemental and Molecular Mimics for Laboratory Studies of Heterogeneous and Multiphase Reactions. *Chem. Soc. Rev.* **2018**, *47* (7), 2374−2400.

(3) Estillore, A. D.; Trueblood, J. V.; Grassian, V. H. Atmospheric Chemistry of Bioaerosols: Heterogeneous and Multiphase Reactions with Atmospheric Oxidants and Other Trace Gases. *Chem. Sci.* **2016**, *7* (11), 6604−6616.

(4) Schiffer, J. M.; Mael, L. E.; Prather, K. A.; Amaro, R. E.; Grassian, V. H. Sea Spray Aerosol: Where Marine Biology Meets Atmospheric Chemistry. *ACS Cent. Sci.* **2018**, *4*, 1617.

(5) Lewis, E. R.; Schwartz, S. E. Sea Salt Aerosol Production: Mechanisms, Methods, Measurements and Models. *Geophys. Monogr.* **2004**, *152*, 413.

(6) Patterson, J. P.; Collins, D. B.; Michaud, J. M.; Axson, J. L.; Sultana, C. M.; Moser, T.; Dommer, A. C.; Conner, J.; Grassian, V. H.; Stokes, M. D.; Deane, G. B.; Evans, J. E.; Burkart, M. D.; Prather, K. A.; Gianneschi, N. C. Sea Spray Aerosol Structure and Composition Using Cryogenic Transmission Electron Microscopy. *ACS Cent. Sci.* **2016**, *2* (1), 40−47.

(7) Wang, X.; Sultana, C. M.; Trueblood, J.; Hill, T. C. J.; Malfatti, F.; Lee, C.; Laskina, O.; Moore, K. A.; Beall, C. M.; McCluskey, C. S.; Cornwell, G. C.; Zhou, T.; Cox, J. L.; Pendergraft, M. A.; Santander, M. V.; Bertram, T. H.; Cappa, C. D.; Azam, F.; DeMott, P. J.; Grassian, V. H.; Prather, K. A. Microbial Control of Sea Spray Aerosol Composition: A Tale of Two Blooms. *ACS Cent. Sci.* **2015**, *1* (3), 124−131.

(8) Cochran, R. E.; Laskina, O.; Trueblood, J. V.; Estillore, A. D.; Morris, H. S.; Jayarathne, T.; Sultana, C. M.; Lee, C.; Lin, P.; Laskin, J.; Laskin, A.; Dowling, J. A.; Qin, Z.; Cappa, C. D.; Bertram, T. H.; Tivanski, A. V.; Stone, E. A.; Prather, K. A.; Grassian, V. H. Molecular Diversity of Sea Spray Aerosol Particles: Impact of Ocean Biology on Particle Composition and Hygroscopicity. *Chem.* **2017**, *2* (5), 655−667.

(9) Pryor, S. C.; Sørensen, L. L. Nitric Acid−Sea Salt Reactions: Implications for Nitrogen Deposition to Water Surfaces. *J. Appl. Meteorol.* **2000**, *39* (5), 725−731.

(10) Trueblood, J. V.; Estillore, A. D.; Lee, C.; Dowling, J. A.; Prather, K. A.; Grassian, V. H. Heterogeneous Chemistry of Lipopolysaccharides with Gas-Phase Nitric Acid: Reactive Sites and Reaction Pathways. *J. Phys. Chem. A* **2016**, *120* (32), 6444−6450.

(11) Aurell, C. A.; Wistrom, A. O. Critical Aggregation Concentrations of Gram-Negative Bacterial Lipopolysaccharides (LPS). *Biochem. Biophys. Res. Commun.* **1998**, *253* (1), 119−123.

(12) Wu, E. L.; Engström, O.; Jo, S.; Stuhlsatz, D.; Yeom, M. S.; Klauda, J. B.; Widmalm, G.; Im, W. Molecular Dynamics and NMR Spectroscopy Studies of E. Coli Lipopolysaccharide Structure and Dynamics. *Biophys. J.* **2013**, *105* (6), 1444−1455.

(13) Thoma, J.; Abuillan, W.; Furikado, I.; Habe, T.; Yamamoto, A.; Gierlich, S.; Kaufmann, S.; Brandenburg, K.; Gutsmann, T.; Konovalov, O.; Inoue, S.; Tanaka, M. Specific Localisation of Ions in Bacterial Membranes Unravels Physical Mechanism of Effective Bacteria Killing by Sanitiser. *Sci. Rep.* **2020**, *10* (1), 1−12.

(14) Coughlin, R. T.; Haug, A.; McGroarty, E. J. Physical Properties of Defined Lipopolysaccharide Salts. *Biochemistry* **1983**, *22* (1978), 2007−2013.

(15) Garidel, P.; Rappolt, M.; Schromm, A. B.; Howe, J.; Lohner, K.; Andrä, J.; Koch, M. H. J.; Brandenburg, K. Divalent Cations Affect Chain Mobility and Aggregate Structure of Lipopolysaccharide from

Salmonella Minnesota Reflected in a Decrease of Its Biological Activity. *Biochim. Biophys. Acta, Biomembr.* **2005**, *1715* (2), 122−131.
(16) Schneck, E.; Schubert, T.; Konovalov, O. V.; Quinn, B. E.; Gutsmann, T.; Brandenburg, K.; Oliveira, R. G.; Pink, D. A.; Tanaka, M. Quantitative Determination of Ion Distributions in Bacterial Lipopolysaccharide Membranes by Grazing-Incidence X-Ray Fluorescence. *Proc. Natl. Acad. Sci. U. S. A.* **2010**, *107* (20), 9147−9151.
(17) Coughlin, R. T.; Tonsager, S.; McGroarty, E. J. Quantitation of Metal Cations Bound to Membranes and Extracted Lipopolysaccharide of Escherichia Coli. *Biochemistry* **1983**, *22* (8), 2002−2007.
(18) Parikh, S. J.; Chorover, J. Infrared Spectroscopy Studies of Cation Effects on Lipopolysaccharides in Aqueous Solution. *Colloids Surf., B* **2007**, *55* (2), 241−250.
(19) Gard, E. E.; Mayer, J. E.; Morrical, B. D.; Dienes, T.; Fergenson, D. P.; Prather, K. A. Real-Time Analysis of Individual Atmospheric Aerosol Particles: Design and Performance of a Portable ATOFMS. *Anal. Chem.* **1997**, *69* (20), 4083−4091.
(20) Garner, J.; Park, K. Chemically Modified Natural Polysaccharides to Form Gels. In *Polysaccharides*; Springer International Publishing: Cham, 2015; pp 1555−1582. DOI: 10.1007/978-3-319-16298-0_31.
(21) Herrmann, M.; Schneck, E.; Gutsmann, T.; Brandenburg, K.; Tanaka, M. Bacterial Lipopolysaccharides Form Physically Cross-Linked, Two-Dimensional Gels in the Presence of Divalent Cations. *Soft Matter* **2015**, *11*, 6037.
(22) Prather, K. A.; Bertram, T. H.; Grassian, V. H.; Deane, G. B.; Stokes, M. D.; Demott, P. J.; Aluwihare, L. I.; Palenik, B. P.; Azam, F.; Seinfeld, J. H.; Moffet, R. C.; Molina, M. J.; Cappa, C. D.; Geiger, F. M.; Roberts, G. C.; Russell, L. M.; Ault, A. P.; Baltrusaitis, J.; Collins, D. B.; Corrigan, C. E.; Cuadra-Rodriguez, L. A.; Ebben, C. J.; Forestieri, S. D.; Guasco, T. L.; Hersey, S. P.; Kim, M. J.; Lambert, W. F.; Modini, R. L.; Mui, W.; Pedler, B. E.; Ruppel, M. J.; Ryder, O. S.; Schoepp, N. G.; Sullivan, R. C.; Zhao, D. Bringing the Ocean into the Laboratory to Probe the Chemical Complexity of Sea Spray Aerosol. *Proc. Natl. Acad. Sci. U. S. A.* **2013**, *110* (19), 7550−7555.
(23) McMurry, P. A Review of Atmospheric Aerosol Measurements. *Atmos. Environ.* **2000**, *34* (12−14), 1959−1999.
(24) Denton, J. K.; Kelleher, P. J.; Johnson, M. A.; Baer, M. D.; Kathmann, S. M.; Mundy, C. J.; Wellen Rudd, B. A.; Allen, H. C.; Choi, T. H.; Jordan, K. D. Molecular-Level Origin of the Carboxylate Head Group Response to Divalent Metal Ion Complexation at the Air−Water Interface. *Proc. Natl. Acad. Sci. U. S. A.* **2019**, *116* (30), 14874−14880.
(25) Jayarathne, T.; Sultana, C. M.; Lee, C.; Malfatti, F.; Cox, J. L.; Pendergraft, M. A.; Moore, K. A.; Azam, F.; Tivanski, A. V.; Cappa, C. D.; Bertram, T. H.; Grassian, V. H.; Prather, K. A.; Stone, E. A. Enrichment of Saccharides and Divalent Cations in Sea Spray Aerosol during Two Phytoplankton Blooms. *Environ. Sci. Technol.* **2016**, *50* (21), 11511−11520.
(26) Duce, R. A.; Hoffman, E. J. Chemical Fractionation at the Air/Sea Interface. *Annu. Rev. Earth Planet. Sci.* **1976**, *4* (1), 187−228.
(27) Gaston, C. J.; Furutani, H.; Guazzotti, S. a.; Coffee, K. R.; Bates, T. S.; Quinn, P. K.; Aluwihare, L. I.; Mitchell, B. G.; Prather, K. a. Unique Ocean-Derived Particles Serve as a Proxy for Changes in Ocean Chemistry. *J. Geophys. Res.* **2011**, *116* (18), 1−13.
(28) Creamean, J. M.; Lee, C.; Hill, T. C.; Ault, A. P.; DeMott, P. J.; White, A. B.; Ralph, F. M.; Prather, K. A. Chemical Properties of Insoluble Precipitation Residue Particles. *J. Aerosol Sci.* **2014**, *76*, 13−27.
(29) Passmore, L. A.; Russo, C. J. *Specimen Preparation for High-Resolution Cryo-EM*, 1st ed.; Elsevier Inc.: 2016; Vol. *579*. DOI: 10.1016/bs.mie.2016.04.011.
(30) Booth, D. S.; Avila-Sakar, A.; Cheng, Y. Visualizing Proteins and Macromolecular Complexes by Negative Stain EM: From Grid Preparation to Image Acquisition. *J. Vis. Exp.* **2011**, *58*, 1−7.
(31) Santos, N. C.; Silva, A. C.; Castanho, M. a R. B.; Martins-Silva, J.; Saldanha, C. Evaluation of Lipopolysaccharide Aggregation by Light Scattering Spectroscopy. *ChemBioChem* **2003**, *4* (1), 96−100.
(32) Snyder, S.; Kim, D.; McIntosh, T. J. Lipopolysaccharide Bilayer Structure: Effect of Chemotype, Core Mutations, Divalent Cations, and Temperature. *Biochemistry* **1999**, *38* (33), 10758−10767.
(33) Jo, S.; Kim, T.; Iyer, V. G. V. G.; Im, W. CHARMM-GUI: A Web-Based Graphical User Interface for CHARMM. *J. Comput. Chem.* **2008**, *29* (11), 1859−1865.
(34) Huang, J.; Mackerell, A. D. CHARMM36 All-Atom Additive Protein Force Field: Validation Based on Comparison to NMR Data. *J. Comput. Chem.* **2013**, *34* (25), 2135−2145.
(35) Huang, J.; Rauscher, S.; Nawrocki, G.; Ran, T.; Feig, M.; de Groot, B. L.; Grubmüller, H.; MacKerell, A. D. CHARMM36m: An Improved Force Field for Folded and Intrinsically Disordered Proteins. *Nat. Methods* **2017**, *14* (1), 71−73.
(36) Schneck, E.; Papp-Szabo, E.; Quinn, B. E.; Konovalov, O. V.; Beveridge, T. J.; Pink, D. A.; Tanaka, M. Calcium Ions Induce Collapse of Charged O-Side Chains of Lipopolysaccharides from Pseudomonas Aeruginosa. *J. R. Soc., Interface* **2009**, *6*, S671−8.
(37) Jeworrek, C.; Evers, F.; Howe, J.; Brandenburg, K.; Tolan, M.; Winter, R. Effects of Specific versus Nonspecific Ionic Interactions on the Structure and Lateral Organization of Lipopolysaccharides. *Biophys. J.* **2011**, *100* (9), 2169−2177.
(38) Orellana, M. V.; Matrai, P. A.; Leck, C.; Rauschenberg, C. D.; Lee, A. M.; Coz, E. Marine Microgels as a Source of Cloud Condensation Nuclei in the High Arctic. *Proc. Natl. Acad. Sci. U. S. A.* **2011**, *108* (33), 13612−13617.
(39) Ault, A. P.; Guasco, T. L.; Baltrusaitis, J.; Ryder, O. S.; Trueblood, J. V.; Collins, D. B.; Ruppel, M. J.; Cuadra-Rodriguez, L. a.; Prather, K. A.; Grassian, V. H. Heterogeneous Reactivity of Nitric Acid with Nascent Sea Spray Aerosol: Large Differences Observed between and within Individual Particles. *J. Phys. Chem. Lett.* **2014**, *5* (15), 2493−2500.
(40) Andreae, M. O.; Rosenfeld, D. Aerosol-Cloud-Precipitation Interactions. Part 1. The Nature and Sources of Cloud-Active Aerosols. *Earth-Sci. Rev.* **2008**, *89* (1−2), 13−41.
(41) Collins, D. B.; Ault, A. P.; Moffet, R. C.; Ruppel, M. J.; Cuadra-Rodriguez, L. A.; Guasco, T. L.; Corrigan, C. E.; Pedler, B. E.; Azam, F.; Aluwihare, L. I.; Bertram, T. H.; Roberts, G. C.; Grassian, V. H.; Prather, K. A. Impact of Marine Biogeochemistry on the Chemical Mixing State and Cloud Forming Ability of Nascent Sea Spray Aerosol. *J. Geophys. Res. Atmos.* **2013**, *118* (15), 8553−8565.
(42) McCluskey, C. S.; Hill, T. C. J.; Sultana, C. M.; Laskina, O.; Trueblood, J. V.; Santander, M. V.; Beall, C. M.; Michaud, J. M.; Kreidenweis, S. M.; Prather, K. A.; Grassian, V. H.; DeMott, P. J. A Mesocosm Double Feature: Insights into the Chemical Make-Up of Marine Ice Nucleating Particles. *J. Atmos. Sci.* **2018**, *75* (7), 2405−2423.
(43) Sandhiya, L.; Kolandaivel, P.; Senthilkumar, K. Oxidation and Nitration of Tyrosine by Ozone and Nitrogen Dioxide: Reaction Mechanisms and Biological and Atmospheric Implications. *J. Phys. Chem. B* **2014**, *118* (13), 3479−3490.
(44) Estillore, A.; Morris, H.; Or, V. W.; Lee, H. D.; Alves, M. R.; Marciano, M. A.; Laskina, O.; Qin, Z.; Tivanski, A. V.; Grassian, V. Linking Hygroscopicity and Surface Microstructure of Model Inorganic Salts, Simple and Complex Carbohydrates, and Authentic Sea Spray Aerosol Particles. *Phys. Chem. Chem. Phys.* **2017**, *19* (31), 21101−21111.

https://doi.org/10.1021/acs.jpclett.1c00810
J. Phys. Chem. Lett. 2021, 12, 5023−5029